6th European Conference on Computational Mechanics (ECCM 6)
7th European Conference on Computational Fluid Dynamics (ECFD 7)
11 – 15 June 2018, Glasgow, UK

NUMERICAL PROPOSALS FOR THE SELF-REPAIRING ASSESMENT OF ECC MEMBERS

CĂLIN GR MIRCEA[1], CORNELIA BAERĂ[2], DIDIER SNOECK[3] AND NELE DE BELIE[3]

[1] Technical University of Cluj-Napoca, Civil Engineering Faculty
28 Memorandumului Street, 400114 Cluj-Napoca, Romania
calin.mircea@dst.utcluj.ro and www.utcluj.ro

[2] NIRD URBAN-INCERC, Timişoara Branch
2 Traian Lalescu Street, 300230 Timişoara, Romania
cornelia.baera@incerc-cluj.ro and www.incd.ro

[3] Ghent University, Department of Structural Engineering, Magnel Laboratory for Concrete Research
Tech Lane Ghent Science Park, Campus A, Technologiepark Zwijnaarde 904, B-9052 Ghent, Belgium
didier.snoeck@UGent.be, nele.debelie@UGent.be and www.concrete.ugent.be

Key words: Self-healing, Self-repairing, ECC, Modeling, Regression Analysis.

Abstract. The paper proposes expressions for the self-repairing assessment (i.e., the recovery of the mechanical properties of the material consequent to the self-healing process) obtained by processing through regression analysis the results of four-point-bending tests performed on ECC specimens. ECC mixes design considered varying the fly ash content/cement content and the type of micro-fibers. Four-point-bending tests were performed on reference specimens and pre-cracked and healed specimens, at various ages and with different loading rates. The studied parameters are the first-cracking strength, ultimate flexural strength upon strain hardening, initial tangent Young modulus and ultimate flexural tensile strain as a measurement of the multiple-cracking capability. Finally, power and logarithmic regression expressions are proposed to simulate the recovery of the self-healing parameters.

1 INTRODUCTION

Engineered Cementitious Composites (ECC), also known as flexible strain-hardening cementitious materials, are a versatile category of mortars/micro-concretes reinforced with disperse fibers (e.g. polymeric fibers), and developed in the frame of the so-called family of High Performance Fiber Reinforced Cementitious Composites (HPFRCC). Besides high ductility and high tensile strength, ECC's can be characterized by self-compacting ability, high early strength and self-healing capacity [1]. The remarkable mechanical performance of ECC's, is doubled by a spectacular intrinsic self-healing capacity with an autogenous mechanism governed by physical, chemical and mechanical processes. Furthermore, in the last decade, researchers developed numerical models to simulate the self-healing of the cementitious materials implying various mechanisms. However, there is still little experimental evidence to provide test data necessary to adjust the constitutive relations to the self-healing process under various loading situations and exposure conditions.

2 RESEARCH SIGNIFICANCE

Tensile failure in cementitious composites presumes progressive micro-cracking, debonding, bridging and many other complex processes. Finally these processes will result in a material discontinuity; a crack. The discrete-crack concept is the most suitable to reflect this phenomenon. However, it is very difficult to integrate it in finite element analyses because it implies the use of an interface element simulating the crack behavior between two solid elements. On the other hand, a smeared crack approach considers the cracked zone as a continuum and the description is made by stress-strain relations. There is no doubt that in the terms of a global structural behavior, the smeared crack concept is more convenient to imply, while the discrete crack is useful in detailing.

Many proposals have been made to simulate self-healing processes. Barbero et al. [2] proposed a constitutive model to predict the general response of the self-healing continuum, while Peizhen et al. [3] developed control equations to simulate damage microcrack healing process controlled by surface diffusion. Schimmel & Remmers [4] introduced a three-phase self-healing model: fracture, transport of the healing agents and mechanical strength recovery. Recently, Davies & Jefferson [5] improved a two-phase composite description of the material, with matrix and inclusions. Numerous constitutive models are related to the strength, stiffness and deformational properties, and damage relationships. The paper proposes expressions grounded on experimental evidence for the estimation of the constitutive laws parameters for a self-repairing treatment, for increasing loading rates of the members subjected to pure flexure. The expressions are calibrated by regression analyses and may be considered in the adaptation of the constitutive models to the self-healing process of ECC.

3 MATERIALS AND TECHNIQUES

Three ECC mixes were derived from the reference mixture reported by Snoeck [5] (i.e. mix M_1, shown in Table 1), by varying the fly ash content/cement content in mix M_2 and changing the micro-fibers type in mix M_3.

All mixtures were made with ordinary Portland cement CEM I 52.5N (Holcim, Belgium) and Class F fly ash (OBBC, Belgium). Silica sand with the maximum grain size of 250 μm (D_{50}=170 μm) (Silbelco, Belgium), was used as aggregate.

The high-range water-reducing agent was a polycarboxylate-based superplasticizer Glenium 51 of 35 % concentration (BASF, Germany). In mixes M_1 and M_2, synthetic polyvinyl alcohol (PVA) micro-fibers (Kuraray, Japan) were added in a constant amount of 2 % in volume, with 8 mm cutting length, 1300 kg/m^3 density and 1.2 % mineral oil coating. In the case of mix M_3, polypropylene micro-fibers (Redco, Belgium) were added in the same amount of 2 % in volume. The polypropylene micro-fibers were 6 mm in length, density of 910 kg/m^3 and slightly lubricated with mineral oil.

Table 1: ECC mixes

Mix code	FA/C ratio	Cement (kg/m^3)	Fly ash (kg/m^3)	Binder (kg/m^3)	Sand (kg/m^3)	Water (kg/m^3)	Superplasticizer (kg/m^3)	Fibers (kg/m^3)
M_1	1.0	608	608	1216	426	365	10	26
M_2	2.4	360	864	1224	426	365	7	26
M_3	1.0	608	608	1216	426	365	10	30

Prismatic specimens of size 40x10x160 mm³ were subjected to four-point bending tests. Loading was done by a Walter+Bai DB 250/15 hydraulic system (see Figure 1), the middle third segment (50 mm) of the specimens being subjected to pure flexure. Two series of specimens were considered: the first series (i.e., specimens with index R) was loaded up to failure at the age of 60 days, while the second series (i.e., specimens with index SH) was initially pre-cracked at 28 days by loading up to a tensile strain of 10 mm/m, unloaded and subjected to a self-healing treatment by dry/wet exposure [7], [8] up to the age of 60 days, and finally tested up to failure. Four different loading rates were considered (see Table 2). For each loading rate three specimens for each ECC mix were tested.

Finally the results were processed through regression analysis and models for the self-healing dependency by the loading rate were proposed.

Figure 1: 4-point bending tests arrangement

Table 2. Loading rates for the four point bending tests

Loading rate		Domain corresponding to the loading rate
deflection/time (mm/s)	strain/time (mm/ms)	
0.0011	5.00×10^{-3}	quasi-static
0.0055	2.50×10^{-2}	
0.0276	1.25×10^{-1}	dynamic cyclic (e.g., earthquake action)
0.1200	0.55×10^{-0}	impact (e.g., shock)

4 SELF-REPAIRING INDICATORS

Figure 2 shows the main parameters considered for the self-repairing assessment. The following indicators were estimated in relation with the loading rate:

- The ratio of the cracking stress $\sigma_{cr\_SH}/\sigma_{cr\_R}$;
- The ratio of the peak flexural stress (i.e., flexural strength) $\sigma_{f\_SH}/\sigma_{f\_R}$;
- The ratio between the initial Young modulus of the reloaded SH specimen and of the R specimen E_{0_SH}/E_{0_R};
- The ratio of the ultimate strains $\varepsilon_{fu\_SH}/\varepsilon_{fu\_R}$.

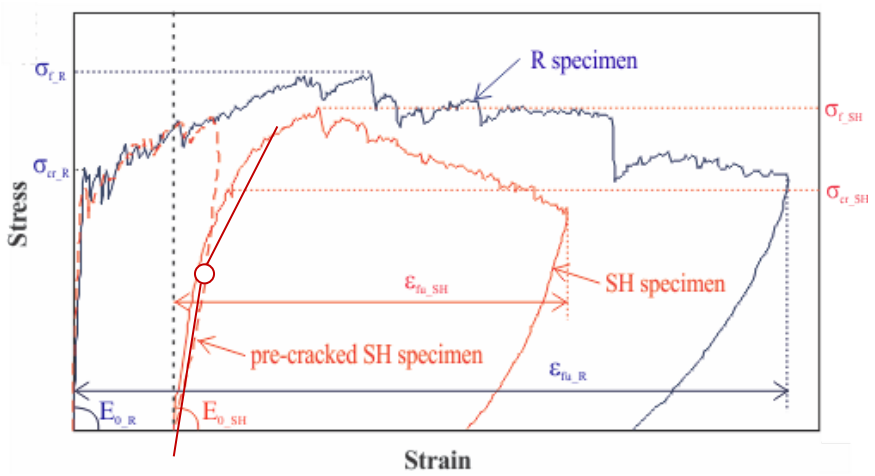

Figure 2: Self-repairing parameters

5 SELF-HEALING ASSESSMENT

The mean values of data recorded for each tested mix were curve-fitted and modeled by the means of regression analysis. Logarithmic, polynomial and power regression functions were considered.

5.1 Strength Indicators

Figures 3 and 4 show the cracking strength recovery for the mixes, related to the applied loading rate. Table 3 shows the associated regression functions and R-squared values. Despite expectancy, power function describes the dependency of the cracking strength by the loading rate better than the logarithmic function. Figure 5 presents the selected regression functions for each ECC mix, and a proposed average that could be used to estimate the cracking strength for a general ECC composition.

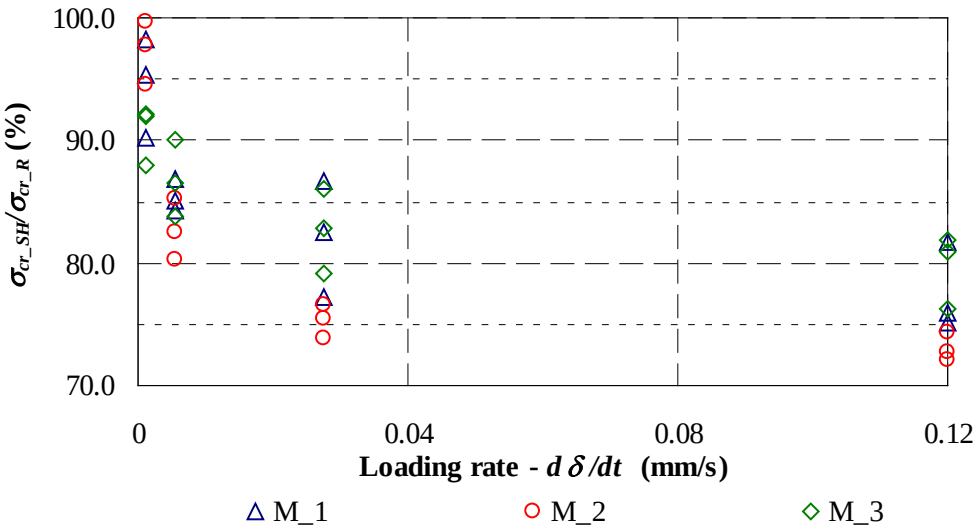

Figure 3: Cracking strength variation with loading regime

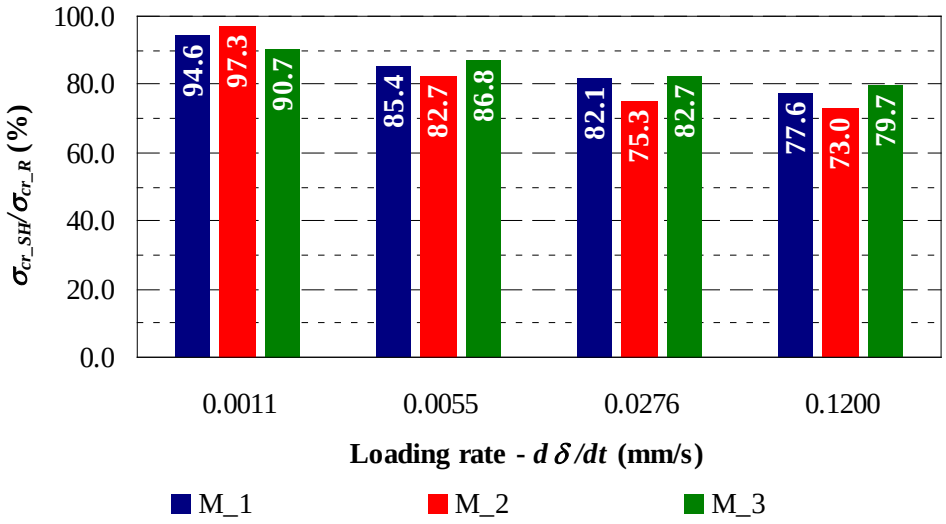

Figure 4: Average cracking strength variation with loading regime

Table 3: Comparative regression functions for the cracking strength

Mix code	Function type	Expression	R-squared value (%)
M_1	logarithmic	$\sigma_{cr\_SH}/\sigma_{cr\_R}$ = -0.03473Ln($d\delta/dt$) + 0.6953	95.34
	polynomial	$\sigma_{cr\_SH}/\sigma_{cr\_R}$ = 28.58($d\delta/dt$)^2 - 4.6195$d\delta/dt$ + 0.9188	82.52
	power	$\sigma_{cr\_SH}/\sigma_{cr\_R}$ = 0.7071($d\delta/dt$)$^{-0.0406}$	96.34
M_2	logarithmic	$\sigma_{cr\_SH}/\sigma_{cr\_R}$ = -0.0514Ln($d\delta/dt$) + 0.5931	90.55
	polynomial	$\sigma_{cr\_SH}/\sigma_{cr\_R}$ = 57.405($d\delta/dt$)^2 – 8.5772$d\delta/dt$ + 0.9336	82.62
	power	$\sigma_{cr\_SH}/\sigma_{cr\_R}$ = 0.6221($d\delta/dt$)$^{-0.0611}$	92.37
M_3	logarithmic	$\sigma_{cr\_SH}/\sigma_{cr\_R}$ = -0.0237Ln($d\delta/dt$) + 0.7448	99.80
	polynomial	$\sigma_{cr\_SH}/\sigma_{cr\_R}$ = 20.378($d\delta/dt$)^2 – 3.2979$d\delta/dt$ + 0.8994	95.42
	power	$\sigma_{cr\_SH}/\sigma_{cr\_R}$ = 0.7502 ($d\delta/dt$)$^{-0.0278}$	99.88

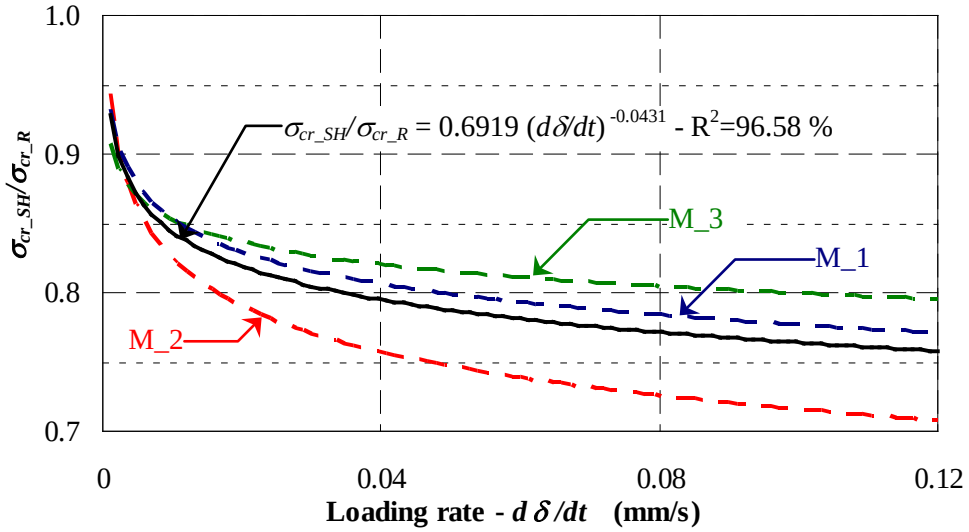

Figure 5: Power regression functions and a general proposal for the cracking strength recovery

Even if physically difficult to interpret, the flexural strength recovery for the mixes, related to the loading applied rate, is presented in Figures 6 and 7. Table 4 shows the associated regression functions and R-squared values. Similar to the recovery of the cracking strength, the best approximation is given by the power function.

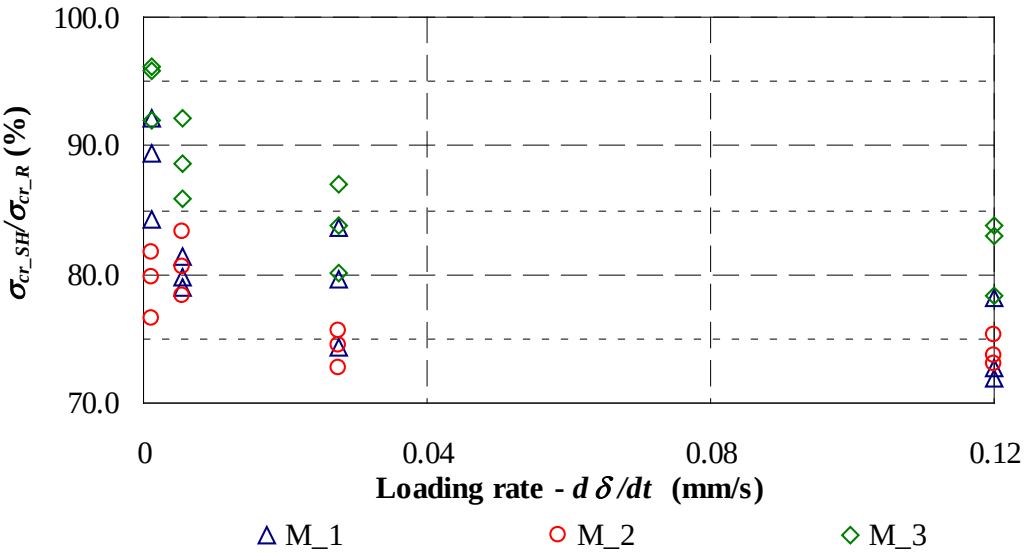

Figure 6: Flexural strength variation with loading regime

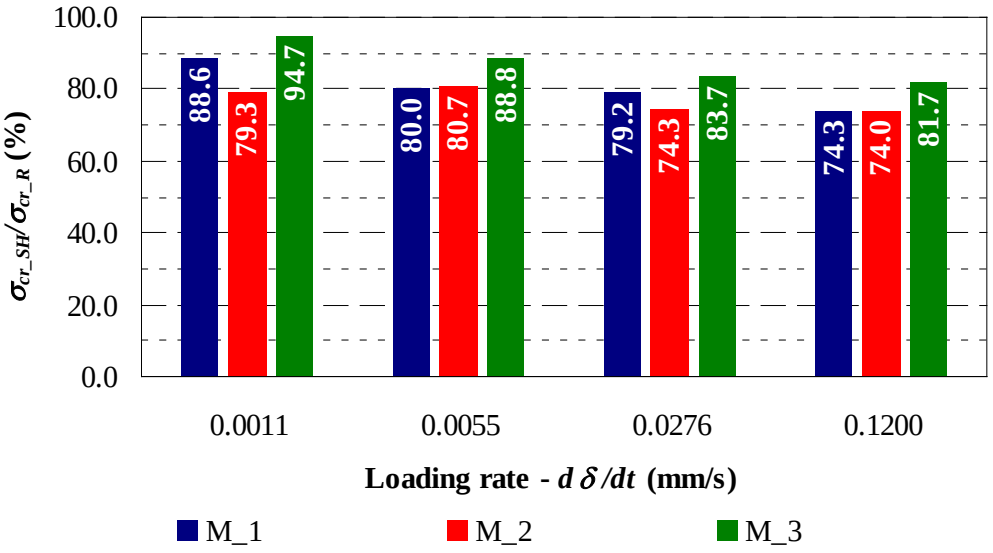

Figure 7: Average flexural strength variation with loading regime

Figure 8 presents the selected regression functions for each ECC mix, and the average proposal that might be used to estimate the recovery of the flexural strength of a generic ECC composition.

Table 4: Comparative regression functions for the flexural strength

Mix code	Function type	Expression	R-squared value (%)
M_1	logarithmic	$\sigma_{cr\_SH}/\sigma_{cr\_R}$ = -0.02794Ln($d\delta/dt$) + 0.6814	90.52
	polynomial	$\sigma_{cr\_SH}/\sigma_{cr\_R}$ = 18.569($d\delta/dt$)^2 – 3.1803$d\delta/dt$ + 0.8573	74.59
	power	$\sigma_{cr\_SH}/\sigma_{cr\_R}$ = 0.69($d\delta/dt$)$^{-0.0344}$	91.33
M_2	logarithmic	$\sigma_{cr\_SH}/\sigma_{cr\_R}$ = -0.0142Ln($d\delta/dt$) + 0.7081	70.55
	polynomial	$\sigma_{cr\_SH}/\sigma_{cr\_R}$ = 18.041($d\delta/dt$)^2 – 2.725$d\delta/dt$ + 0.8076	90.33
	power	$\sigma_{cr\_SH}/\sigma_{cr\_R}$ = 0.7099($d\delta/dt$)$^{-0.0185}$	91.09
M_3	logarithmic	$\sigma_{cr\_SH}/\sigma_{cr\_R}$ = -0.0282Ln($d\delta/dt$) + 0.74741	96.78
	polynomial	$\sigma_{cr\_SH}/\sigma_{cr\_R}$ = 29.399($d\delta/dt$)^2 – 4.5018$d\delta/dt$ + 0.934	91.94
	power	$\sigma_{cr\_SH}/\sigma_{cr\_R}$ = 0.7552 ($d\delta/dt$)$^{-0.0321}$	97.30

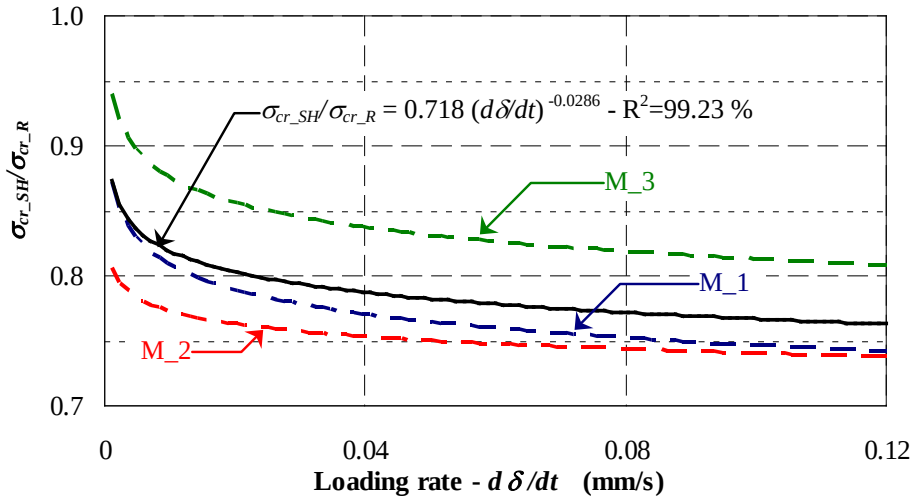

Figure 8: Power regression functions and a general proposal for the flexural strength recovery

5.2 Stiffness Indicator

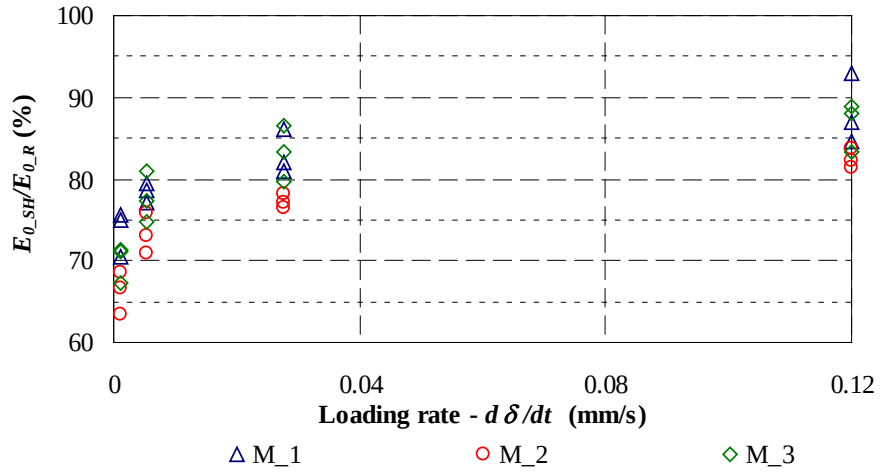

Figure 9: Young modulus variation with loading regime

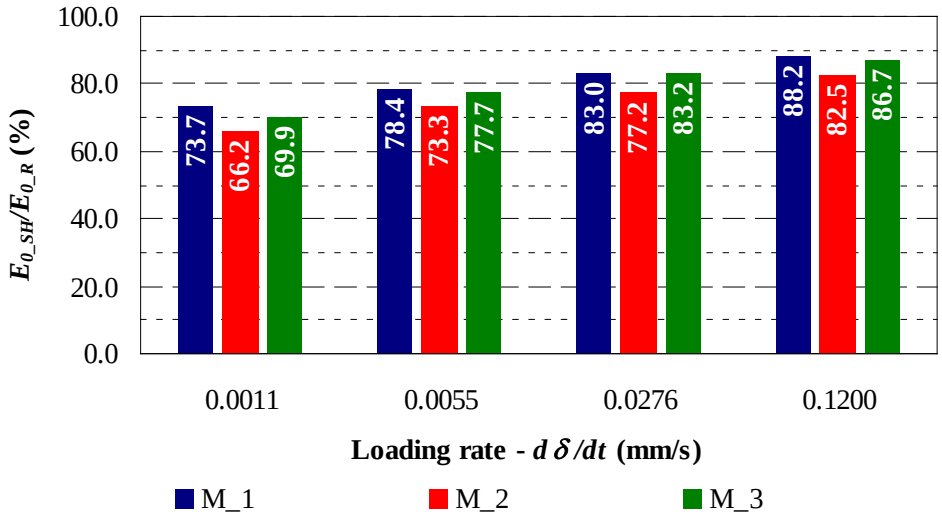

Figure 10: Average initial Young variation with loading regime

Table 5: Comparative regression functions for the initial tangent Young modulus

Mix code	Function type	Expression	R-squared value (%)
M_1	logarithmic	$E_{0\_SH}/E_{0\_R} = 0.0306\text{Ln}(d\delta/dt) + 0.9438$	99.76
	polynomial	$E_{0\_SH}/E_{0\_R} = -21.818(d\delta/dt)^2 + 3.7412 d\delta/dt + 0.747$	95.62
	power	$E_{0\_SH}/E_{0\_R} = 0.954(d\delta/dt)^{+0.0379}$	98.92
M_2	logarithmic	$E_{0\_SH}/E_{0\_R} = 0.0338\text{Ln}(d\delta/dt) + 0.8976$	98.84
	polynomial	$E_{0\_SH}/E_{0\_R} = -25.392(d\delta/dt)^2 + 4.2479 d\delta/dt + 0.6806$	89.75
	power	$E_{0\_SH}/E_{0\_R} = 0.9124(d\delta/dt)^{+0.0456}$	98.26
M_3	logarithmic	$E_{0\_SH}/E_{0\_R} = 0.0359\text{Ln}(d\delta/dt) + 0.9526$	97.78
	polynomial	$E_{0\_SH}/E_{0\_R} = -33.825(d\delta/dt)^2 + 5.3032 d\delta/dt + 0.7178$	90.05
	power	$E_{0\_SH}/E_{0\_R} = 0.9694\ (d\delta/dt)^{+0.0459}$	96.81

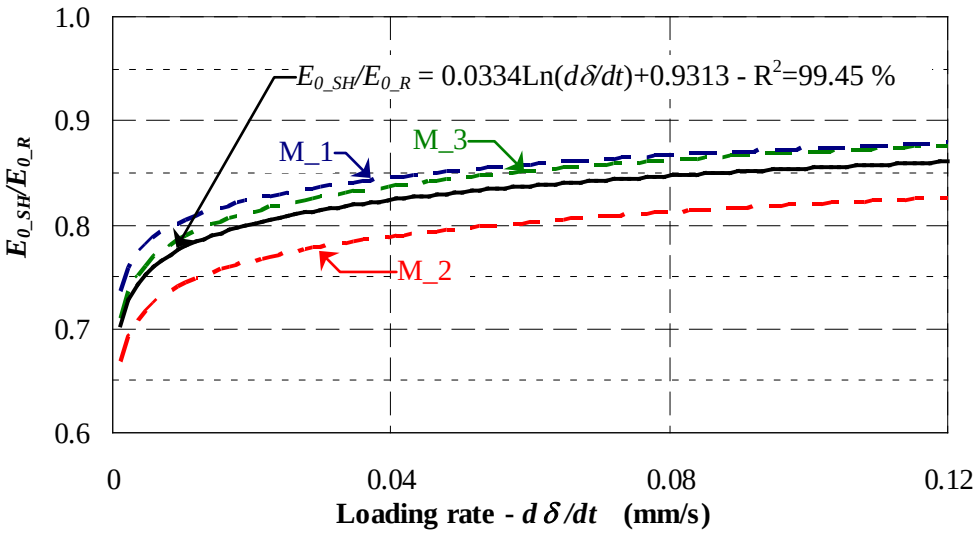

Figure 11: Logarithmic regression functions and a general proposal for the rigidity recovery

Rigidity recovery was analyzed through the tangent initial Young modulus. A similar procedure was applied. Results are shown in Figures 9 and 10. Table 5 presents the regression functions. In the case of the stiffness recovery, logarithmic regression functions were selected and the general proposal is shown in Figure 11.

5.3 Ductility Indicator

The same steps were made for the analysis of the ductility recovery. Results are shown in Figures 12 and 13. Table 6 presents the regression functions and Figure 14 the selected ones, together with the general suggestion of logarithmic type.

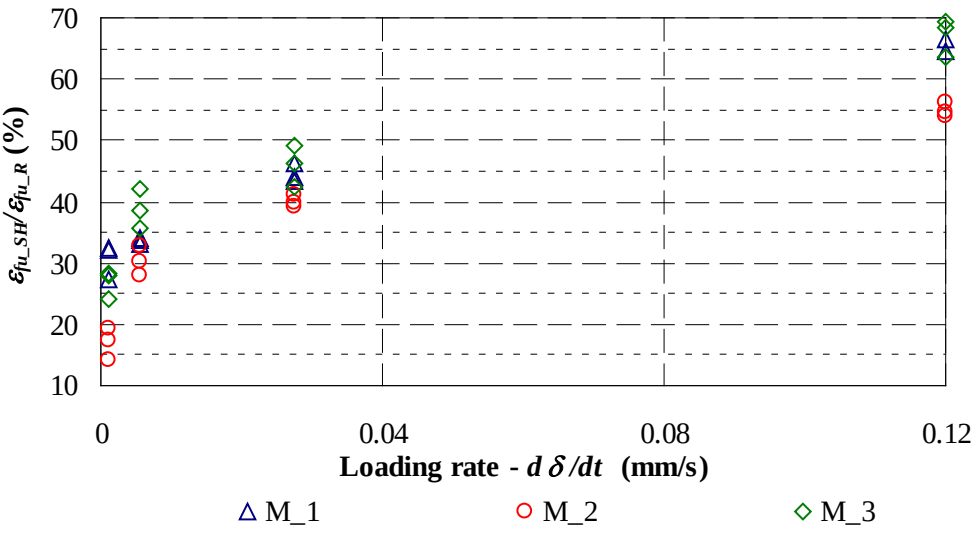

Figure 12: Ultimate strains variation with loading regime

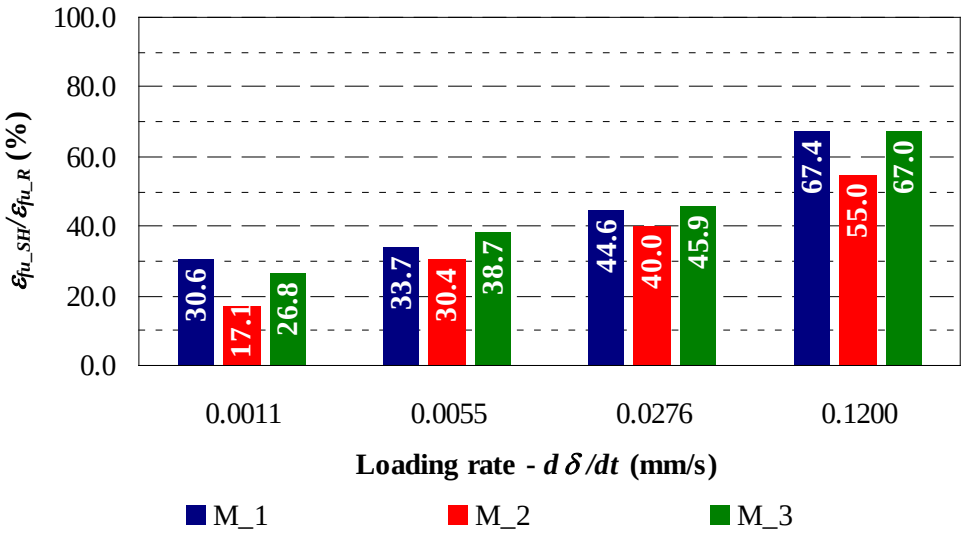

Figure 13: Mean ultimate strains variation with loading regime

Table6: Comparative regression functions for the ultimate strains

Mix code	Function type	Expression	R-squared value (%)
M_1	logarithmic	$\varepsilon_{fu\_SH}/\varepsilon_{fu\_R} = 0.0766\text{Ln}(d\delta/dt) + 0.7804$	96.96
	polynomial	$\varepsilon_{fu\_SH}/\varepsilon_{fu\_R} = -23.25(d\delta/dt)^2 + 5.8837 d\delta/dt + 0.3024$	99.98
	power	$\varepsilon_{fu\_SH}/\varepsilon_{fu\_R} = 0.8826(d\delta/dt)^{+0.1677}$	92.36
M_2	logarithmic	$\varepsilon_{fu\_SH}/\varepsilon_{fu\_R} = 0.0786\text{Ln}(d\delta/dt) + 0.7043$	99.10
	polynomial	$\varepsilon_{fu\_SH}/\varepsilon_{fu\_R} = -50.357(d\delta/dt)^2$ 8.9283$d\delta/dt + 0.2032$	93.38
	power	$\varepsilon_{fu\_SH}/\varepsilon_{fu\_R} = 0.9544(d\delta/dt)^{+0.2419}$	97.34
M_3	logarithmic	$\varepsilon_{fu\_SH}/\varepsilon_{fu\_R} = 0.0812\text{Ln}(d\delta/dt) + 0.8057$	97.78
	polynomial	$\varepsilon_{fu\_SH}/\varepsilon_{fu\_R} = -33.075(d\delta/dt)^2 + 7.0544 d\delta/dt + 0.2996$	95.21
	power	$\varepsilon_{fu\_SH}/\varepsilon_{fu\_R} = 0.9635(d\delta/dt)^{+0.186}$	97.68

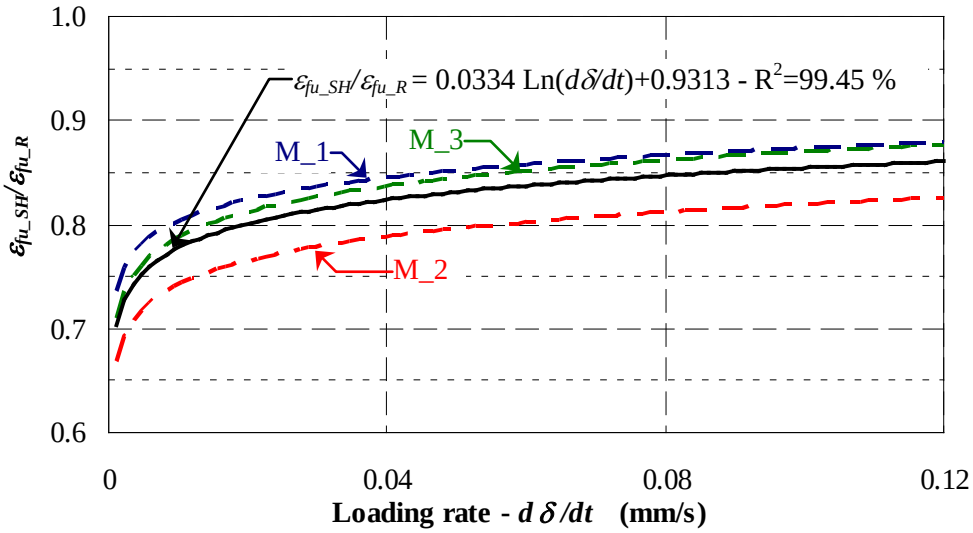

Figure 14: Logarithmic regression functions and a general proposal for the rigidity recovery

6 CONCLUSIONS

This paper presents the recovery prediction of the self-repairing parameters of ECC members subjected to pure flexure with increasing loading rates (i.e., rates corresponding to quasi-static, dynamic cyclic and impact loading), and due to autogenous self-healing. The predictions are made on the ground of four-point bending tests performed on specimens made with three mix compositions, and the processing of the raw data by regression analysis.

The following conclusions can be drawn within the goal of the research:

- The general trend in recovery of the self-repairing parameters is ascending in all three directions of interest: mechanical strength, rigidity and ductility;
- The recovery of the mechanical strength of the ECC members subjected to pure flexure (i.e., cracking and flexural strength) with increasing loading rate follows a decreasing power function pattern;
- The recovery of the stiffness and ductility (i.e., initial Young tangent modulus and ultimate

flexural strain) has increasing trends with the loading rate and are best simulated by logarithmic functions;
- More accurate simulations may be done in the future considering more refined regression functions and more self-repairing parameters in terms of strength and strain.

REFERENCES

[1] Li, V.C., From Micromechanics To Structural Engineering -- The Design Of Cementitious Composites For Civil Engineering Applications, *JSCE J. of Struc. Mechanics and Earthquake Engineering* (1993), **10(2)**: 37-48.

[2] Barbero, E., Greco, F. and Lonetti, P, Continuum damage-healing mechanics with application to self-healing composites. *International Journal of Damage Mechanics* (2005) **14 (1)**: 51–81.

[3] Peizhen, H., Zhonghua, L. and Jun, S. Finite element analysis on evolution process for damage microcrack healing. *Acta Mechanica Sinica* (2000) **16 (3)**: 254–263.

[4] Schimmel, E.C., Remmers, J.J.C. *Development of a Constitutive Model for Self-Healing Materials*. Delft Aerospace Computational Science, Report DACS-06- 003 (2006), 15 p.

[5] Davies, R. and Jefferson, A. Micromechanical modelling of self-healing cementitious materials. *International Journal of Solids and Structures* (2017) **113–114**: 180–191.

[6] Snoeck, D. *Self-healing and microstructure of cementitious materials with microfibres and superabsorbent polymers*. PhD Thesis. Ghent University (2015), 325p.

[7] Snoeck, D., Van Tittelboom, K., Steuperaert, S., Dubruel, P. and De Belie, N. Self-healing cementitious materials by the combination of microfibres and superabsorbent polymers. *Journal of Intelligent Material Systems and Structures* (2014)**, 25(1):** 13-24.

[8] Snoeck, D. and De Belie, N. Repeated autogenous healing in strain-hardening cementitious composites by using superabsorbent polymers. *Journal of Materials in Civil Engineering* (2015), 04015086, 1-11.